Langmuir

Article

pubs.acs.org/Langmuir

Comparison of the Interfacial Activity between Homogeneous and Janus Gold Nanoparticles by Pendant Drop Tensiometry

Miguel Angel Fernandez-Rodriguez,[†] Yang Song,[‡] Miguel Ángel Rodríguez-Valverde,[†] Shaowei Chen,[‡] Miguel Angel Cabrerizo-Vilchez,[†] and Roque Hidalgo-Alvarez*[,†]

[†]Biocolloid and Fluid Physics Group, Applied Physics Department, Faculty of Sciences, University of Granada, 18071 Granada, Spain

[‡]Department of Chemistry and Biochemistry, University of California, 1156 High Street, Santa Cruz, California 95064, United States

ABSTRACT: The interfacial activity of 3.5 nm homogeneous (HPs) and amphiphilic Janus gold nanoparticles (JPs) was characterized by pendant drop tensiometry for water/air and water/decane interfaces. This technique requires a smaller quantity of nanoparticles than the traditional Langmuir balance technique. The direct deposition at the interface of the nanoparticles dispersed in a spreading solvent also requires smaller quantities of sample than does adsorption from the bulk. From the growing and shrinking of the pendant drops, the interfacial activity of the nanoparticles can be evaluated and compared within a wide range of area per particle. In this work, the JPs exhibited a higher interfacial activity than did the HPs in all cases. A hard disk model fits the piecewise compression isotherm of the HPs, yet this model underestimates the interactions between the JPs adsorbed at the interface.

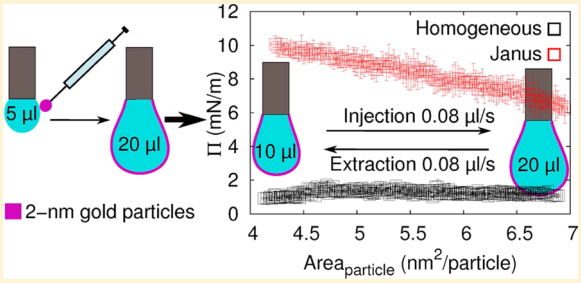

INTRODUCTION

Janus nanoparticles are anisotropic colloidal entities with two regions of different physicochemical properties. This anisotropy can lead to the spontaneous self-assembly of nanoparticles or can be responsive to an external stimulus such as a magnetic or electric field, pH or temperature gradients, and so forth.[1,2] Depending on the particular anisotropy of the nanoparticles, they cover a wide range of applications such as biosensors,[2] drug delivery and immunotherapy,[3] water-repellent textiles,[4] and nanoparticles that become aligned in an external electric or magnetic field.[5−7]

Janus nanoparticles with a wettability anisotropy can be used to stabilize Pickering emulsions. Unlike homogeneous nanoparticles, amphiphilic Janus nanoparticles can exhibit a high interfacial activity regardless of the degree of amphiphilicity because of the spatial separation of the different wettability regions.[8] Thus, amphiphilic Janus-like gold nanoparticles functionalized with thiol-terminated poly(ethylene glycol) chains and short alkane thiols have been used as water/oil emulsion stabilizers because they rearrange when placed at the interface.[9] Moreover, Janus gold nanoparticles half functionalized with polydopamine show that the electrostatic repulsion between nanoparticles determines the resulting particle self-assembly at water/oil interfaces as a result of the hydrophilic polydopamine and hydrophobic gold faces of each particle.[10] In addition, micrometer-sized Janus gold−silica nanoparticles have been found to stabilize water/oil emulsions for longer than 1 year, compared to 2 h of demulsification when homogeneous silica nanoparticles were used.[11] Importantly, not only does the wettability contrast of the Janus nanoparticles condition the interfacial activity but also their morphology controls the interfacial activity at a given water/oil interface, which determines the packing behavior of the Janus nanoparticles.[12] Therefore, nonspherical emulsion droplets have been obtained by using Janus nanoparticles with asymmetrical morphology.[13]

There are different synthesis strategies involving bulk methods in which the Janus nanoparticles are synthesized in a solvent, usually one pot methods.[6,9,14] However, other strategies involve the particles being placed at a given liquid interface to be functionalized,[15,16] usually resulting in noticeably smaller quantities of Janus nanoparticles than in bulk methods. The Langmuir film balance technique is widely used to characterize the interfacial activity and arrangement of nanoparticles at water/air and water/oil interfaces.[16−20] Another experimental approach is to use growing/shrinking drop tensiometry[21,22] because the quantity of nanoparticles required is much smaller than for a standard Langmuir film balance experiment. Nevertheless, a certain number of nanoparticles are still necessary for the experiments that involve the adsorption of Janus nanoparticles at the interface of a pendant drop from the bulk.[2,15,23,24] When the amount of sample available is insufficient for studying the adsorption from the bulk to the interface of the pendant drop, the direct deposition of nanoparticles at the pendant drop interface from a volatile solvent allows the study of the interfacial activity. Moreover, solvent evaporation is a violent and rapid process that helps the nanoparticles to be adsorbed at the interface of the pendant drop, faster than diffusion from the bulk toward

Received: October 30, 2013
Revised: January 27, 2014
Published: February 3, 2014

   dx.doi.org/10.1021/la404194e | *Langmuir* 2014, 30, 1799−1804

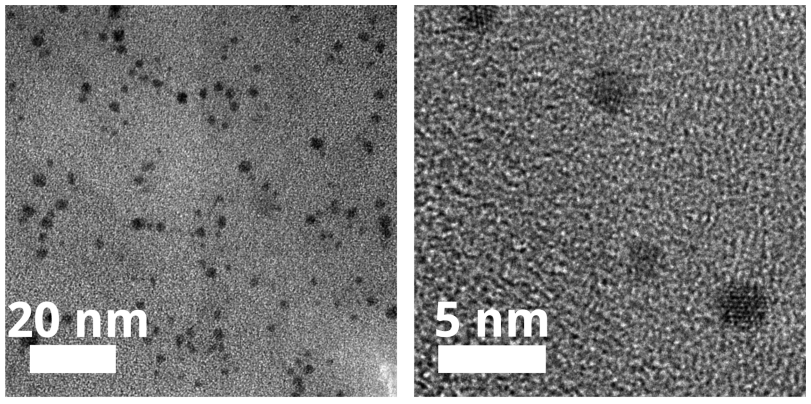

Figure 1. (a) High-resolution TEM micrograph of the JPs studied. (b) High-resolution TEM micrograph of the JPs at higher magnification.

the pendant drop interface.[25] This technique enables us to control the number of nanoparticles deposited at the pendant drop interface.

The simplest model used to describe the interfacial arrangement of the nanoparticles at the interface is the hard disk model in which the nanoparticles are represented by hard entities placed at the interface. The nanoparticles do not interact when there is enough room for every nanoparticle, but they become close packed when the area per particle is sufficiently low.[26] However, when the nanoparticles are functionalized with large polymers, Monte Carlo simulations and experimental data show complex behavior compared to that of hard objects at liquid/liquid interfaces.[27]

In this study, we characterized the interfacial activity of 3.5-nm-diameter homogeneous gold nanoparticles capped with hexanethiol and Janus gold nanoparticles with hydrophobic hexanethiolates on one hemisphere and hydrophilic 2-(2-mercapto-ethoxy)ethanol on the other. The pendant drop technique enabled the study of the interfacial activity of those particles at the water/air and water/decane interfaces. Moreover, because of the small number of nanoparticles available, the nanoparticles dispersed in a volatile solvent were directly deposited at the pendant drop water/air interface using a microsyringe. By the controlled deposition of a desired number of nanoparticles at the pendant drop interface and subsequent shrinkage−growth cycles of the pendant drop, we studied the different interfacial arrangements of nanoparticles for different values of the drop area available per nanoparticle.

MATERIALS AND METHODS

Sample Preparation. Homogeneous gold nanoparticles capped with hexanethiol (HPs) were synthesized following Brust's protocol.[28] Janus gold nanoparticles (JPs) were synthesized by functionalizing a hemisphere of the HPs with 2-(2-mercapto-ethoxy)ethanol (MEE) using Chen's protocol.[16,20] The terminal groups were $-CH_3$ and $-OH$ for the hexanethiol- and MEE-functionalized hemispheres, respectively. The Janus morphology of JPs was thoroughly evaluated by Chen and co-workers in references 16, 20, and 29. They reported contact angle measurements of nanoparticle ensembles,[16] AFM adhesion force measurements of individual nanoparticles,[29] and NOESY NMR measurements of the polarization interactions between neighboring spins of the nanoparticle surface capping ligands.[16] The wettability differences between hexanethiol and MEE terminal groups suggest interfacial activity of the JPs. Both nanoparticles were redispersed separately in tetrahydrofuran (THF) as the spreading agent. The JP diameter quantified from high-resolution TEM micrographs of the isolated nanoparticles was 3.5 ± 0.9 nm (Figure 1a,b).

Electrophoretic Mobility. The electrophoretic mobility of both HPs and JPs was measured with a Zetasizer Nano device (Malvern) in a 10^{-2} M sodium citrate Milli-Q water solution, and these were the values found: $\mu_{e,HP} = (-1.1 \pm 0.7) \times 10^{-8}$ m^2/(V·s) and $\mu_{e,JP} = (-2.2 \pm 1.5) \times 10^{-8}$ m^2/(V·s). The 1:1 electrolyte added to the nanoparticle solutions enabled the measurement of stable mobility values because the electrical double layer of both nanoparticles was fairly stabilized.

Growing and Shrinking Pendant Drop. We used a homemade pendant drop tensiometer[30] that enables a change in the drop volume and area using a microinjector (Hamilton). The volume of a water pendant drop, usually in the range of 10 to 30 μL, allows us to work with smaller quantities of nanoparticle rather than the higher working volumes of the traditional Langmuir balance tensiometer.[16−20] The growth and shrinkage of the pendant drop volume enables different nanoparticle arrangements at the interface once a fixed number of nanoparticles is adsorbed. Real time drop images are processed by the axisymmetric drop shape analysis profile (ADSA-P),[31] providing the pendant drop area and surface tension. Water/oil interfaces can be explored with the pendant drop tensiometer readily by submerging the pendant drop in oil. In this study, as-received decane (Sigma-Aldrich) was used as the oil phase.

To perform a growing and shrinking pendant drop experiment, first it is necessary to adsorb the nanoparticles at the drop interface. Usually, the experiments are performed with adsorption of nanoparticles from the bulk to the pendant drop interface,[2,12,23,24] but when the quantity of nanoparticles available is insufficient for this kind of study, the direct deposition of the desired number of nanoparticles in a spreading solvent at the interface with a microsyringe is an alternative. In this study, the spreading solvent used was THF and the deposition was performed on the surface of a 5 μL Milli-Q water pendant drop in air with a 5 μL microsyringe (Hamilton) and a micropositioner. Immediately after the deposition of the nanoparticles, the surface tension decreased markedly because of the spreading solvent. While the THF was evaporating, the volume of the pendant drop was slowly increased at 0.08 μL/s up to the final 20 μL volume and maintained until the surface tension was stable. Thereby, this process avoided the fall of the pendant drop due to the abrupt decrease in the surface tension because of the spreading solvent effect on the interface. For higher volumes of spreading solvent, to avoid the drop fall it was necessary to perform a 10 μL stabilization step before the final growth up to 20 μL. In all cases, the evaporation of the spreading solvent ensured that the nanoparticles had enough energy to adsorb at the interface, compared to the slow process of adsorption from the bulk.[25] In Figure 2, we can observe the surface tension evolution over time after the JP deposition at the water/air interface. The procedure followed is illustrated with a visual scheme.

The growing and shrinking pendant drop experiment was performed with slightly different protocols for water/air or water/

dx.doi.org/10.1021/la404194e | Langmuir 2014, 30, 1799−1804

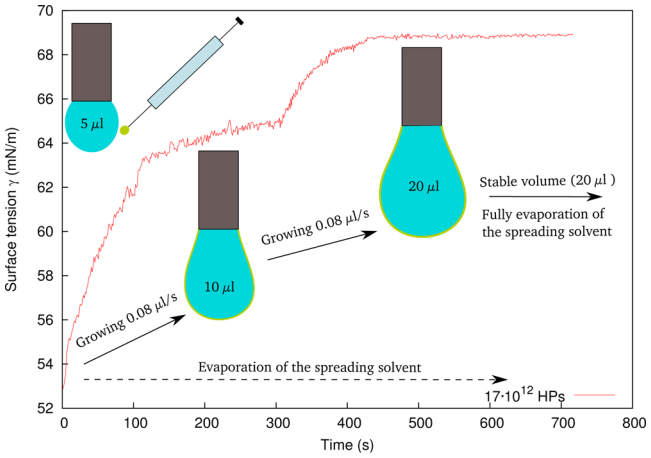

Figure 2. Surface tension evolution over time for JP deposition at the surface of a initial 5 μL Milli-Q water pendant drop and subsequent growth to 20 μL at a 0.08 μL/s rate. After complete solvent evaporation, the surface tension remained stable.

decane interfaces. For both water/air and water/decane interfaces, the shrinking and growing volume rate was 0.08 μL/s but the volume range was 20 μL ↔ 10 μL for water/air and 30 μL ↔ 10 μL for water/decane interfaces because the pendant drop was larger when immersed in decane before the drop fall. Additionally, the volume was decreased up to 5 μL prior to the immersion of the water pendant drop in decane to avoid the drop fall. For each particle concentration, the shrinkage was repeated three times and the growth was repeated twice. The surface pressure $\Pi = \gamma_0 - \gamma$, where γ_0 is the surface tension of the phase without nanoparticles and γ is the measured surface tension, is plotted against the area of the pendant drop divided by the number of deposited nanoparticles. A growing and shrinking pendant drop experiment is illustrated in Figure 3.

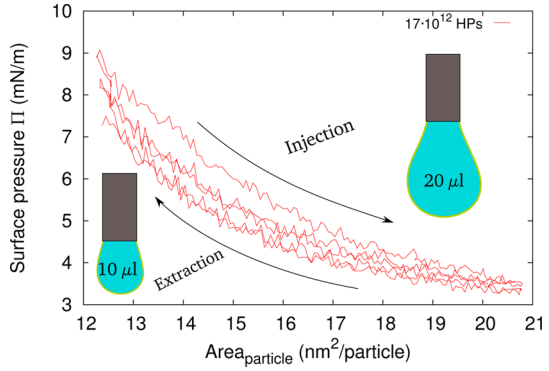

Figure 3. Surface pressure against area per particle for a growing and shrinking pendant drop experiment at the water/decane interface. The pendant drop volume was changed to between 30 and 10 μL at a 0.08 μL/s rate. The growth was repeated three times and the shrinkage twice. The reproducibility between growth and shrinkage repetitions and the low hysteresis of the cycle are remarkable.

RESULTS AND DISCUSSION

The direct deposition of the JPs and HPs at the water/air interface produced a decrease in the surface tension once the spreading solvent was fully evaporated. The surface tension evolution over time for different amounts of HPs and JPs deposited at the drop surface is plotted in Figure 4. The stable values of surface tension after the spreading solvent evaporation are compiled in Table 1. The surface tension decreased as the

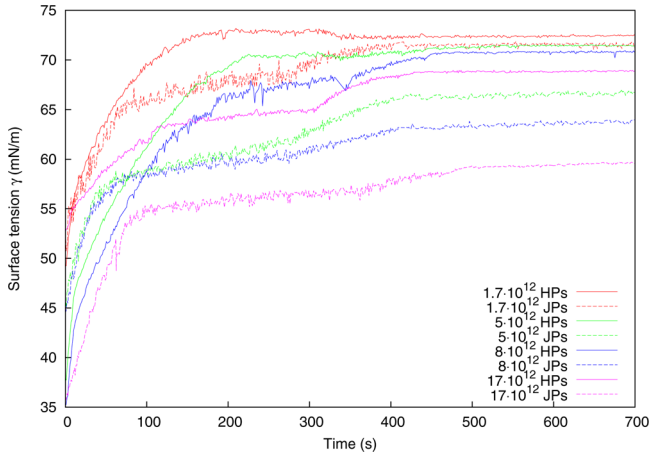

Figure 4. Surface tension evolution over time after the deposition of HPs and JPs at the surface of a initial 5 μL Milli-Q water pendant drop and subsequent growth up to 20 μL at a 0.08 μL/s rate. Each line corresponds to different depositions with different amounts of HPs and JPs, respectively. After solvent evaporation, the surface tension remained stable.

Table 1. Stable Surface Tension after the Spreading Solvent Evaporation for Different Numbers of Deposited HPs and JPs

deposited particles	γ_{HP} (mN/m)	γ_{JP} (mN/m)
1.7×10^{12}	72.40 ± 0.07	71.5 ± 0.3
5×10^{12}	71.38 ± 0.11	66.7 ± 0.3
8×10^{12}	70.78 ± 0.10	63.7 ± 0.3
17×10^{12}	68.84 ± 0.06	59.50 ± 0.20

nanoparticle concentration increased. This decrease is greater for JPs than for HPs, suggesting an enhanced interfacial activity of the JPs as compared to the HPs.[32]

The Pickering emulsions become increasingly stabilized with increasing particle size. In this context, small nanoparticles (~100 nm) need to be tightly anchored at the interface to avoid desorption.[2] The adsorption energy at the interface is on the order of k_BT when the nanoparticle diameter is in the range of a few nanometers.[23] Thus, the 3.5-nm-diameter HPs and JPs were expected to be expelled from the pendant drop interface because of thermal fluctuations or even by the drop shrinkage.[33] Although the drop surface revealed visible aggregates and noticeable opacity as the nanoparticle concentration increased (Figure 5), both HPs and JPs exhibited a significant and stable effect on the surface tension after THF evaporation. This suggests that a significant number of nanoparticles did not desorb from the drop interface over time. From molecular dynamics, Udayana-Ranatunga et al.[34] suggest that ligand rearrangement contributes significantly to the energetics of nanoparticles at interfaces.

Because of the experimental limitations in the drop area range reproduced with a single growth and shrinkage experiment, several growth and shrinkage experiments were performed for different numbers of deposited nanoparticles to probe a wider range of area per particle. Results for the growing and shrinking pendant drop experiments at the water/air and water/decane interfaces are plotted in Figure 6 for different concentrations of HPs and JPs. We averaged the different growth and shrinkage cycles for each nanoparticle concentration because of the low hysteresis. It can be seen that the surface pressure increased as the area per particle decreased for

dx.doi.org/10.1021/la404194e | Langmuir 2014, 30, 1799−1804

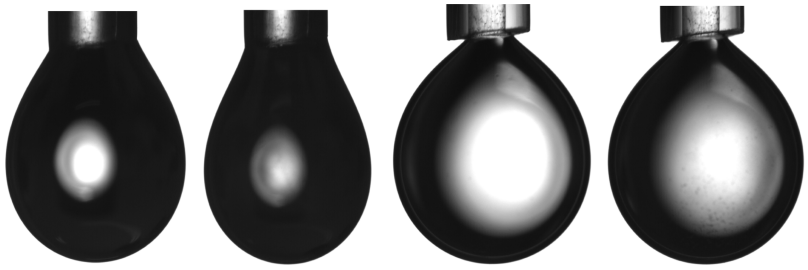

(a) $1.7{\cdot}10^{12}$ JPs in water/air (b) $17{\cdot}10^{12}$ JPs in water/air (c) $1.7{\cdot}10^{12}$ JPs in water/decane (d) $17{\cdot}10^{12}$ JPs in water/decane

Figure 5. Images of pendant drops with different concentrations of JPs and at different interfaces. The pendant drop volumes were 20 and 30 μL for the water/air and water/decane interfaces, respectively.

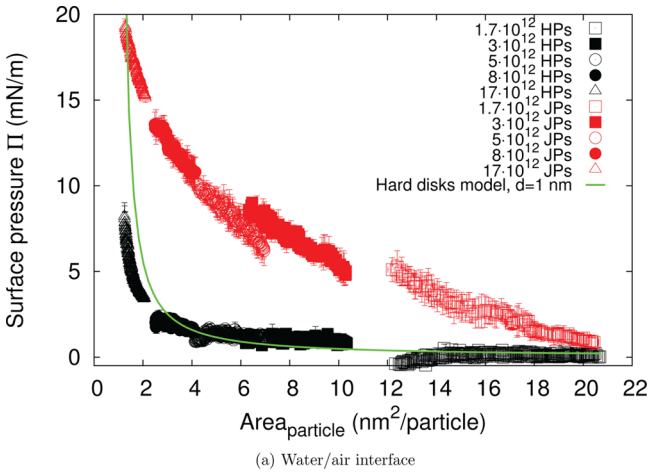

(a) Water/air interface

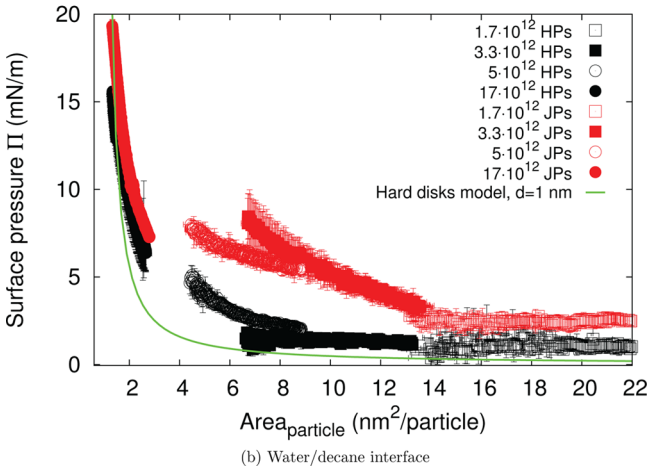

(b) Water/decane interface

Figure 6. Surface pressure against area per particle for different numbers of HPs (black symbols) and JPs (red symbols) deposited at the interface. Each black or red symbol corresponds to a single HP or JP deposition at the interface of the pendant drop, respectively. The solid line is the hard disk model (eq 1) for disks of 1 nm diameter.

both JPs and HPs. The interfacial activity reached similar values with both types of nanoparticles for the most expanded interfacial states (i.e., highest values of area per particle, >18 nm^2/particle). However, the interfacial activity was higher with the JPs than with the HPs for the most compressed states (<2 nm^2/particle) where the surface pressure was 2.5 times higher for the JPs than for the HPs at the water/air interface and 1.2 times higher at the water/decane interface. At both interfaces, the JPs reached the same surface pressure: 19.3 ± 0.4 mN/m for the most compressed interfacial state. The higher interfacial activity of HPs at the water/decane interface for the most compressed state may reveal that the HPs move more freely in the presence of the decane phase because of its affinity for hydrophobic particles. This nanoparticle mobility allowed us to realize arrangements with greater interfacial coverage and higher surface pressure.

Different models were explored to fit the experimental data with a hypothetical piecewise compression isotherm. A model based on the repulsion between charged particles[35] results in negligible surface pressure resulting from the low effective electric charge of HPs and JPs, with its small size and effective charge. Moreover, the short chains of the hexanethiol and MEE capping ligands did not require a large polymer correction.[27] The simply scaled particle theory of the hard disks model[26] is in reasonable agreement with the HP results for both water/air and water/decane interfaces for hard disks with 1 nm diameter (Figure 6). In the hard disk model, the surface pressure II for a given area per particle at the interface $A_{particle}$ is written as follows

$$\Pi(A_{particle}) = \frac{k_B T}{A_{particle}\left(1 - \frac{\pi d^2}{4A_{particle}}\right)^2} \quad (1)$$

where k_B is the Boltzmann constant, T is the temperature, and d is the hard disk diameter. The hard disk model predicts no interactions when there is enough room for all nanoparticles at the interface and a significant effect on the surface tension at high concentrations when the nanoparticles are near close-packed. The fitted diameter of 1 nm points out that not all of the nanoparticles were really adsorbed at the interface or that they were aggregated. In such a situation, the number of particles at the interface was smaller than expected, and it is necessary to shrink the pendant drop further to reach the close-packed regime, resulting in a lower effective diameter of the hard disk model. This simple model underestimates the results of surface pressure against area per particle for the JPs. Further models taking into account the interaction between the Janus nanoparticles are needed to explain the results. Such models should incorporate the role of the wettability contrast between the two hemispheres of the JPs, with the low effective charge and steric interactions between these nanoparticles.

Although there is evidence that not all nanoparticles are uniformly distributed at the pendant drop interface (visible aggregates in Figure 5 and underestimated effective diameter for the HPs as discussed before), the nanoparticles placed at the interface seem to be well anchored at both the water/air and water/decane interfaces because the different growth and shrinkage cycles for a given nanoparticle concentration show a

dx.doi.org/10.1021/la404194e | Langmuir 2014, 30, 1799−1804

very low hysteresis value, pointing out that the nanoparticles did not desorb from the interface as the drop area was changed. From these results, the JPs exhibited enhanced interfacial activity as compared to the HPs.

CONCLUSIONS

The interfacial activity of homogeneous 3.5 nm gold nanoparticles capped with hexanethiol and Janus 3.5 nm gold nanoparticles capped half with hexanethiol and half with MEE was explored using pendant drop tensiometry. The direct deposition of the nanoparticles in a spreading solvent at the interface of the pendant drop with a microsyringe rendered it possible to explore the surface tension evolution over time as the spreading solvent was evaporating at different nanoparticle concentrations. The direct deposition needed only a small quantity of nanoparticles in contrast to the conventional adsorption of nanoparticles from the pendant drop bulk or a conventional Langmuir balance experiment. The growing and shrinking pendant drop technique allowed us to study the surface pressure for a wide range of area per nanoparticle at the water/air and water/decane interfaces by varying the drop area and the number of nanoparticles deposited on the drop surface. For both interfaces studied, the homogeneous nanoparticles showed lower interfacial activity than the Janus nanoparticles. A hard disk model could fit the experimental results for the homogeneous particles, but it underestimated the interaction between the Janus nanoparticles at the interface.

AUTHOR INFORMATION

Corresponding Author

*E-mail: rhidalgo@ugr.es.

Notes

The authors declare no competing financial interest.

ACKNOWLEDGMENTS

This study was supported by the Junta de Andalucía (projects P09-FQM-4698 and P10-FQM-5977), the Ministerio de Economía y Competitividad (project MAT2011-23339) and the U.S. National Science Foundation (DMR-0804049). We thank Dr. J. A. Holgado-Terriza for the Contacto software used for surface tension measurements.

REFERENCES

(1) Yoshida, M.; Lahann, J. Smart Nanomaterials. *ACS Nano* **2008**, *2*, 1101−1107.

(2) Walther, A.; Müller, A. H. E. Janus Particles: Synthesis, Self-Assembly, Physical Properties, and Applications. *Chem. Rev.* **2013**, *113*, 5194−5261.

(3) Kaewsaneha, C.; Tangboriboonrat, P.; Polpanich, D.; Eissa, M.; Elaissari, A. Janus Colloidal Particles: Preparation, Properties, and Biomedical Applications. *ACS Appl. Mater. Interfaces* **2013**, *5*, 1857−1869.

(4) Synytska, A.; Khanum, R.; Ionov, L.; Cherif, C.; Bellmann, C. Water-Repellent Textile via Decorating Fibers with Amphiphilic Janus Particles. *ACS Appl. Mater. Interfaces* **2011**, *3*, 1216−1220.

(5) Bormashenko, E.; Bormashenko, Y.; Pogreb, R.; Gendelman, O. Janus Droplets: Liquid Marbles Coated with Dielectric/Semiconductor Particles. *Langmuir* **2011**, *27*, 7−10.

(6) Teo, B. M.; Suh, S. K.; Hatton, T. A.; Ashokkumar, M.; Grieser, F. Sonochemical Synthesis of Magnetic Janus Nanoparticles. *Langmuir* **2011**, *27*, 30−33.

(7) Yuet, K. P.; Hwang, D. K.; Haghgooie, R.; Doyle, P. S. Multifunctional Superparamagnetic Janus Particles. *Langmuir* **2010**, *26*, 4281−4287.

(8) Binks, B. P.; Fletcher, P. D. I. Particles Adsorbed at the Oil-Water Interface: A Theoretical Comparison between Spheres of Uniform Wettability and Janus Particles. *Langmuir* **2001**, *17*, 4708−4710.

(9) Larson-Smith, K.; Pozzo, D. C. Pickering Emulsions Stabilized by Nanoparticle Surfactants. *Langmuir* **2012**, *28*, 11725−11732.

(10) Xu, H.; Liu, X.; Su, G.; Zhang, B.; Wang, D. Electrostatic Repulsion-Controlled Formation of Polydopamine-Gold Janus Particles. *Langmuir* **2012**, *28*, 13060−13065.

(11) Fujii, S.; Yokoyama, Y.; Miyanari, Y.; Shiono, T.; Ito, M.; Yusa, S.-i.; Nakamura, Y. Micrometer-Sized Gold Silica Janus Particles as Particulate Emulsifiers. *Langmuir* **2013**, *29*, 5457−5465.

(12) Ruhland, T. M.; Grüschel, A. H.; Ballard, N.; Skelhon, T. S.; Walther, A.; Müller, A. H. E.; Bon, S. A. F. Influence of Janus Particle Shape on Their Interfacial Behavior at Liquid-Liquid Interfaces. *Langmuir* **2013**, *29*, 1388−1394.

(13) Meng, X.; Guan, Y.; Zhang, Z.; Qiu, D. Fabrication of a Composite Colloidal Particle with Unusual Janus Structure as a High-Performance Solid Emulsifier. *Langmuir* **2012**, *28*, 12472−12478.

(14) Zhang, J.; Jin, J.; Zhao, H. Surface-Initiated Free Radical Polymerization at the Liquid-Liquid Interface: A One-Step Approach for the Synthesis of Amphiphilic Janus Silica Particles. *Langmuir* **2009**, *25*, 6431−6437.

(15) Liu, L.; Ren, M.; Yang, W. Preparation of Polymeric Janus Particles by Directional UV-Induced Reactions. *Langmuir* **2009**, *25*, 11048−11053.

(16) Pradhan, S.; Xu, L.; Chen, S. Janus Nanoparticles by Interfacial Engineering. *Adv. Funct. Mater.* **2007**, *17*, 2385−2392.

(17) Detrich, Á.; Deák, A.; Hild, E.; Kovács, A. L.; Hórvölgyi, Z. Langmuir and Langmuir-Blodgett Films of Bidisperse Silica Nanoparticles. *Langmuir* **2010**, *26*, 2694−2699.

(18) Kim, J. Y.; Raja, S.; Stellacci, F. Evolution of Langmuir Film of Nanoparticles Through Successive Compression Cycles. *Small* **2011**, *7*, 2526−2532.

(19) Sashuk, V.; Hołyst, R.; Wojciechowski, T.; Fiałkowski, M. Close-Packed Monolayers of Charged Janus-Type Nanoparticles at the Air-Water Interface. *J. Colloid Interface Sci.* **2012**, *375*, 180−186.

(20) Pradhan, S.; Brown, L.; Konopelski, J.; Chen, S. Janus Nanoparticles: Reaction Dynamics and NOESY Characterization. *J. Nanopart. Res.* **2009**, *11*, 1895−1903.

(21) Xu, H.; Melle, S.; Golemanov, K.; Fuller, G. Shape and Buckling Transitions in Solid-Stabilized Drops. *Langmuir* **2005**, *21*, 10016−10020.

(22) Monteux, C.; Kirkwood, J.; Xu, H.; Jung, E.; Fuller, G. G. Determining the Mechanical Response of Particle-Laden Fluid Interfaces Using Surface Pressure Isotherms and Bulk Pressure Measurements of Droplets. *Phys. Chem. Chem. Phys.* **2007**, *9*, 6344−6350.

(23) Ferdous, S.; Ioannidis, M.; Henneke, D. Adsorption Kinetics of Alkanethiol-Capped Gold Nanoparticles at the Hexane-Water Interface. *J. Nanopart. Res.* **2011**, *13*, 6579−6589.

(24) Ruhland, T. M.; Gröschel, A. H.; Walther, A.; Müller, A. H. E. Janus Cylinders at Liquid-Liquid Interfaces. *Langmuir* **2011**, *27*, 9807−9814.

(25) Garbin, V.; Crocker, J. C.; Stebe, K. J. Nanoparticles at Fluid Interfaces: Exploiting Capping Ligands to Control Adsorption, Stability and Dynamics. *J. Colloid Interface Sci.* **2012**, *387*, 1−11.

(26) Santos, A.; López de Haro, M.; Yuste, S. An Accurate and Simple Equation of State for Hard Disks. *J. Chem. Phys.* **1995**, *103*, 4622−4625.

(27) Isa, L.; Amstad, E.; Schwenke, K.; Del Gado, E.; Ilg, P.; Kroger, M.; Reimhult, E. Adsorption of Core-Shell Nanoparticles at Liquid-Liquid Interfaces. *Soft Matter* **2011**, *7*, 7663−7675.

(28) Brust, M.; Walker, M.; Bethell, D.; Schiffrin, D. J.; Whyman, R. Synthesis of Thiol-Derivatised Gold Nanoparticles in a Two-Phase Liquid-Liquid System. *J. Chem. Soc., Chem. Commun.* **1994**, *0*, 801−802.

(29) Xu, L.-P.; Pradhan, S.; Chen, S. Adhesion Force Studies of Janus Nanoparticles. *Langmuir* **2007**, *23*, 8544−8548.

(30) Wege, H.; Holgado-Terriza, J.; Galvez-Ruiz, M.; Cabrerizo-Vilchez, M. Development of a new Langmuir-Type Pendant-Drop Film Balance. *Colloids Surf., B* **1999**, *12*, 339−349.
(31) Montes Ruiz-Cabello, F.; Rodriguez-Valverde, M.; Cabrerizo-Vilchez, M. Contact Angle Hysteresis on Polymer Surfaces: An Experimental Study. *J. Adhes. Sci. Technol.* **2011**, *25*, 2039−2049.
(32) Glaser, N.; Adams, D. J.; Böker, A.; Krausch, G. Janus Particles at Liquid-Liquid Interfaces. *Langmuir* **2006**, *22*, 5227−5229.
(33) Garbin, V.; Crocker, J. C.; Stebe, K. J. Forced Desorption of Nanoparticles from an Oil−Water Interface. *Langmuir* **2012**, *28*, 1663−1667.
(34) Udayana Ranatunga, R. J. K.; Kalescky, R. J. B.; Chiu, C.-c.; Nielsen, S. O. Molecular Dynamics Simulations of Surfactant Functionalized Nanoparticles in the Vicinity of an Oil/Water Interface. *J. Phys. Chem. C* **2010**, *114*, 12151−12157.
(35) Aveyard, R.; Clint, J.; Nees, D.; Paunov, V. Compression and Structure of Monolayers of Charged Latex Particles at Air/Water and Octane/Water Interfaces. *Langmuir* **2000**, *16*, 1969−1979.